doi.org/10.36721/PJPS.2025.38.4.REG.13601.1

A novel approach to urease inhibition and antioxidant therapeutics by using AgNPs-doped TiO_2NPs stabilized by short chain pyrazole carbothioamide derivatives

Rafia Usman Khan[1], Faiza Saleem[2], Mehreen Lateef[3], Anjum Ayub[1]*, Saman Fatima[1], Huzifa Ahmed[1], Hassan Munir[1] and Khalid Mohammed Khan[2]

[1]Department of Chemistry, NED University of Engineering and Technology, Karachi, Pakistan
[2]H.E.J. Research Institute of Chemistry, International Center for Chemical and Biological Sciences, University of Karachi, Karachi, Pakistan
[3]Department of Biochemistry, Multi-Disciplinary Research Laboratory, Bahria University, Karachi, Pakistan

Abstract: This study details our approach to the synthesis, characterization and applications of silver nanoparticles (AgNPs) doped titanium dioxide nanoparticles (TiO_2NPs). Prior to doping both the nanoparticles AgNPs and TiO_2NPs were stabilized by a new small chain 5-(3-Nitrophenyl) Hydrazono-2-Pyridine-4,5-Dihydro-1H-Pyrazole-1-Thioamide (PDPC). The PDPC's small alkyl chain demonstrated efficient modulation over the growth dynamics and structural characteristics of AgNPs doped TiO_2NPs system. An extensive study of the electronic and photonic properties of PDPC-stabilized (AgNPs) integrated into (TiO_2NPs) was conducted utilizing advanced methods such as ultraviolet-visible absorption spectroscopy, atomic force microscope and fourier-transform IR. The atomic force microscopy (AFM) analysis revealed the morphology of the PDPC-stabilized (AgNPs) incorporated into (TiO_2NPs), with an average diameter measured at 3±1 nm. The synthesized PDPC-stabilized (AgNPs) doped with (TiO_2NPs) demonstrated significant antioxidant activity, achieving 82 ± 0.01% inhibition, alongside notable urease inhibition, with an efficacy of 80 ± 0.53% inhibition. Additionally, this composite system was effective in the reduction of Para-nitrophenol (PNP) and Methylene-blue (MB) dye. The integration of PDPC-stabilized AgNPs doped TiO_2NPs facilitated the rapid transformation of p-nitrophenol and Methylene-blue into p-aminophenol (p-Amp) and leuco Methylene-blue (LMB) within one second, utilizing sodium borohydride ($NaBH_4$) at normal temperature and pressure conditions demonstrated a kinetic behavior typical of pseudo-first-order reactions.

Keywords: Para-aminophenol, heterogeneous catalysis, 5-(3-nitrophenyl) hydrazono-2-pyridine-4,5-dihydro-1h-pyrazole-1-thioamide stabilizer, doped silver nanoparticles, urease inhibition, anti-oxidant

Submitted on 25-10-2024 – Revised on 26-12-2024– Accepted on 09-01-2025

INTRODUCTION

The realm of nanotechnology deals with engineering and applying materials that are smaller than 100 nanometers. At the nano scale, the properties and behavior of materials can differ from those at larger scales. Consequently, nanotechnology can be utilized in various fields such as electronics, energy, medicine, textiles and materials science. One of the unique features of nanotechnology is its capacity to produce novel materials and devices with exceptional properties (Talebian *et al.,* 2021). Nano materials can be categorized based on their morphology, size and other characteristics, including carbon, polymer, semiconductor, metal and lipid based nano materials. They find applications in various industrial sectors, such as pharmaceuticals, biomedical, catalysis, wastewater treatment and energy storage (Nagar *et al.,* 2020).

So far, the semiconductor-based (Zhu *et al.,* 2021) TiO_2NPs have been demonstrated to be the most advantageous and efficient photo catalyst due to their distinctive characteristics, such as photochemical stability, non-toxicity, affordability and high effectiveness (Naidoo *et al.,* 2021). In addition, they possess unique optical, electronic and magnetic properties and a high refractive index (n = 2.4), which makes them suitable for various purposes such as coatings, medicines, inks, textiles, cosmetics and food products. Furthermore, there is some evidence that TiO_2NPs may have oxidation inhibitor properties due to their capacity to scavenge free radicals (Nilavukkarasi *et al.,* 2021, Kocić, *et al.,* 2022). The fields of antioxidants reveal several critical gaps that hinder their therapeutic potential. A primary concern is stability and bioavailability; traditional antioxidants such as coenzyme Q10 (ubiquinone) can degrade rapidly under physiological conditions. Cur cumin also (Giuseppe *et al.,* 2024) has demonstrated antioxidant properties, its inability to effectively cross the blood-brain barrier limits its therapeutic impact on neuro degeneration. This situation underscores the urgent need for safer, more effective alternatives that not only enhance stability and bioavailability but also provide targeted action against

**Corresponding author:* e-mail: anjumayub@neduet.edu.pk

specific oxidative stress pathways, paving the way for more effective treatments in various diseases.

In addition, Urease enzyme is essential for the decomposition of urea, a waste product excreted in urine. Current urease inhibitors face significant challenges that limit their clinical effectiveness. For instance, phenylphosphorodiamidate (PPD) (Luzia V Modolo., *et al,* 2018) has been widely studied as a urease inhibitor; however, its efficacy is often compromised by metabolic degradation and poor solubility. Numerous studies have suggested that TiO_2NPs have been found to possess urease inhibition properties, which could be helpful in the removal of urea from wastewater ((Liu *et al.,* 2022, Wag mode *et al.,* 2019).

In addition, TiO_2NPs possess photo catalytic properties that make them a promising tool for reducing environmental pollutants through a process known as photo catalysis. The reaction pathway involving Para-nitrophenol (PNP) and Methylene-blue (MB) culminates in the formation of aminophenol (p-Amp) and leuco Methylene-blue (LMB) respectively. For example, in the case of *p*-nitrophenol, the TiO_2NPs can adsorb the pollutant on its surface and convert it to aminophenol by transferring an electron from the electron-hole pair to the *p*-nitrophenol molecule. Similarly, the TiO_2NPs can adsorb the dye on their surface for Methylene-blue and reduce it to leucomethylene by accepting an electron from the electron-hole pair (Kianfar *et al.,* 2020).

Though there have many advantages for TiO_2 compared to other semiconductor photocatalysts, its wide electronic band gap of around 3.20 eV restricts its effectiveness and overall performance in sunlight are limited, as it can only absorb UV light. Doping of TiO_2NPs with a noble metal, especially with silver nanoparticles (AgNPs), can significantly increase UV-Visible absorbance due to the surface plasmon resonance (SPR) effect. Distinctive chemical, physical and biological properties of AgNPs have made them a topic of growing interest in recent times (Muthukrishnan *et al.,* 2023). AgNPs extends the optical absorption range of the material into the visible light spectrum or near-infrared radiation, which improves photo catalytic efficiency by facilitating the separation and transmission of photo-induced electrons and holes (Caglar *et al.,* 2023, Yerli-Soylu *et al.,* 2022).

Controlling the size of metal nanoparticles during synthesis is crucial in determining their physical and chemical characteristics. Stabilizers are essential among these factors in modulating the size of metal nanoparticles and keeping their stability by passivating and reducing the high surface charge of metal nanoparticles, thus preventing further growth and aggregation (Trinh *et al.,* 2023, Thukkaram *et al.,* 2020).

Adding innovative dimensions to nanomaterial chemistry, we report the synthesis of pyrazole 5-(3-Nitrophenyl) Hydrazono - 2 - Pyridine - 4,5 - Dihydro - 1H-Pyrazole-1-Thioamide (PDPC) with a short heterocyclic chain that strongly stabilizes AgNPs-doped TiO_2NPs nanoparticles. The PDPC structure has a rigid backbone chain that effectively stabilizes AgNPs-doped TiO_2NPs nanoparticles by strong chemisorption of the carbothioamide group with the nanoparticles (Madkour *et al.,* 2021, George, *et al.,* 2022). PDPC, a pyrazole derivative, is an organic compound that has been studied for its potential applications in medicinal chemistry. Several studies have shown that PDPC exhibits significant antimicrobial and anti-inflammatory properties and it has been explored as a potential lead compound for developing new molecules to treat bacterial infections and inflammatory diseases. Additionally, pyrazole derivatives have shown potential as an antitumor agent and have been investigated for their ability to inhibit cancer cell proliferation. Overall, this compound is a crucial molecule in drug discovery and may have significant therapeutic applications in the future (Monti *et al.,* 2022, Grala, M *et al.,* 2023).The synthesized nano-composite systems, featuring PDPC-stabilized AgNPs doped TiO_2NPs demonstrated significant biological efficacy and served as effective heterogeneous catalysts for environmental purposes.

MATERIALS AND METHODS

General methods and techniques

All experimental solvents and chemicals regents were sourced from Fanara Chemicals and Sigma Aldrich Co., used as they were provided. Sensitive reactions were conducted in a nitrogen atmosphere. Unless specified otherwise, distilled water was utilized to prepare all experimental solutions. Silver nitrate ($AgNO_3$), titanium (IV) oxide powder ACS reagent, ≥ 99.0% Sigma Aldrich), p-nitrophenol (PNP)($O_2NC_6H_4OH$, Merck), Methylene-blue (MB) ($C_{16}H_{18}ClN_3S.xH_2O$, Merck) was used as a pollutant. Mass spectra were obtained using the MAT 312 and MAT 113D mass spectrometers. For 1H-NMR analysis, a Bruker Avance Neo spectrometer operating at 400 MHz was employed. Ultraviolet-Visible absorption and Fourier Transform Infrared Spectroscopy spectra were captured using the Shimadzu FTIR8900 and Bruker Vector22 instruments. The size of the PDPC-stabilized AgNPs doped in TiO_2NPs, was measured with an Agilent Technologies AFM 5500.

Procedure for the synthesis of (E)-3-(3-nitrophenyl)-1-(pyridin-2-yl)-prop-2-en-1-one (Azachalcone)

To prepare “azachalcone” an intermediate, a combination of 5 mmol of 3-nitrobenzaldehyde and 5 mmol of 2-acetylpyridine was dissolved in methyl alcohol (30 mL) in a round-bottom flask (100 mL). After that round-bottom flask was subsequently placed in a container filled with ice. Several drops of concentrated NaOH solution were added to maintain the pH of the reaction mixture at an alkaline

level at 0°C. The development of the reaction mixture was examined using thin-layer chromatography (TLC) at 30-minute intervals, during which a precipitate began to form. A trace amount of concentrated HCl were added to stop the further reaction. After obtaining the raw product, it was filtered and thoroughly rinsed with an ample amount of distilled water. Following the drying process, the product was then used in the next stage of the procedure (Saleem *et al.,* 2021).

Procedure for the synthesis of 5-(-3-nitrophenyl)-3-(-pyridin-2-yl)-4,5-dihydro-1H-pyrazole-1-thioamide (PDPC)

A heated solution of (E)-3-(3-nitrophenyl)-1-(pyridin-2-yl)-prop-2-en-1-one (1 mmol) in 10 mL of absolute ethanol was stirred in the presence of an aqueous potassium hydroxide solution. An equivalent amount of thiosemicarbazide (1 mmol) was subsequently added to the mixture. The reaction was kept under reflux for a duration of three hours, while thin-layer chromatography (TLC) provided continuous monitoring. Once all starting materials had completely reacted, the resultant precipitates were filtered and washed with distill water. To obtain the desired compound, they were subsequently crystallized from ethanol, 5-(3-Nitrophenyl) Hydrazono-2-Pyridine-4,5-Dihydro-1H-Pyrazole-1-Thioamide (PDPC)

Spectral characterization of 5-(3-Nitrophenyl) hydrazono-2-Pyridine-4,5-dihydro-1H-pyrazole-1-thioamide (PDPC)

Yield: 83%; ^{1}H-NMR (400 MHz, DMSO-d_6): δ 8.59 (d, $J_{6,5}$ = 4.4 Hz, 1H, H-6), 8.30 (d, $J_{4',5'}$ = 8.0 Hz, 1H, H-4'), 8.28 (s, 1H, H-2'), 8.14 (broad s, 1H, NH), 8.09 (ovp, 1H, H-5'), 7.97 (broad s, 1H, NH), 7.91 (td, $J_{4(5,3)}$ = 8 Hz, $J_{4,6}$ = 2 Hz, 1H, H-4), 7.63 (d, $J_{6',5'/3,4}$ = 5.2 Hz, 2H, H-6', H-3), 7.45 (dd, $J_{5,4}$ = 6.8 Hz, $J_{5,6}$ = 5.2 Hz, 1H, H-5), 6.09 (dd, $J_{c,b}$ = 12 Hz, $J_{c,a}$ = 4 Hz, 1H, H-c), 4.00 (dd, $J_{b,a}$ = 18.4 Hz, $J_{b,c}$ = 11.6 Hz, 1H, H-b), 3.22 (dd, $J_{a,b}$ = 18.8 Hz, $J_{a,c}$ = 4 Hz, 1H, H-a); EI MS *m/z* (% rel. abund.): 327 (M^+, 22), 310 (37), 293 (18), 222 (23), 171 (100), 146 (42), 78 (23).

Preparation of PDPC-stabilized AgNPs.

Under slow stirring, in a glass vial, 30 mL of distilled water was taken. To this, 50 µL of fresh 100 mM $AgNO_3$ aqueous and 10 µL of PDPC derivative stabilizer were added; then, 50 µL of fresh 100 mM $NaBH_4$ aqueous were added drop-wise. Consequently, the solution turned from colorless to yellowish, indicating the formation of PDPC-stabilized AgNPs.

Preparation of PDPC-stabilized AgNPs-doped TiO_2NPs

Under slow stirring, 420 mg of titanium dioxide were slowly added to a vial containing 1 mL of distilled water. Placed it on a stirrer at 30 °C for 1 minute at 250 rpm to obtain a slurry and then 5 μL (PDPC) stabilizer was added to the slurry and stirred for a further 1 minute. After that, 1 mL of AgNPs-$NaBH_4$-PDPC (mentioned above) was added to the slurry and for 5 minutes stirred it. This slurry was then dried in the oven at 60 °C until the dried powder was formed.

UV- Visible analysis of PDPC-stabilized AgNPs-doped TiO_2NPs

The confirmation of 5-(3-nitrophenyl)-3-(pyridin-2-yl)-4,5-dihydro-1H-pyrazole-1-thioamide (PDPC) stabilized AgNPs-doped TiO_2NPs through the observation of surface plasmon resonance (SPR) was achieved by analyzing absorbance shown characteristic SPR peak of the PDPC-TiO_2NPs system at 280 nm, PDPC- $NaBH_4$-AgNPs at 405 nm and PDPC-stabilized AgNPs-doped TiO_2NPs at 490 nm.

FTIR analysis of PDPC-stabilized AgNPs-doped TiO_2NPs

Fourier Transform IR (FTIR) was conducted to verify the synthesis of PDPC-stabilized AgNPs-doped TiO_2NPs. The spectra were plotted within the wavenumber range of 500 to 4000 cm^{-1}.

Surface structure of PDPC-stabilized AgNPs-doped TiO_2NPs

The surface structure of the fabricated PDPC-stabilized AgNPs-doped TiO_2NPs was analyzed using atomic force microscopy (AFM). For the examination, the sample was affixed to a stub using double-sided adhesive tape after it had been lyophilized and dispersed.

Method of urease inhibition of PDPC control

The free radical scavenging activity was measured by 1,1-diphenyl-2-picryl-hydrazil (DPPH) using the method described by Gulcin *et al* (1). The reaction mixtures were created by mixing 25 µL of Jack bean urease solution with 55 µL of buffer and 100 mM urea. These mixtures were then incubated with 5 µL of 1 mM PDPC control compound at 30 °C for 15 minutes in 96-well plates. Urease activity was evaluated by measuring ammonia production using the indophenol method outlined by Weatherburn. Each well received 45 µL of phenol reagent (consisting of 1% w/v phenol and 0.005% w/v sodium nitroprusside) and 70 µL of alkali reagent (made of 0.5% w/v NaOH and 0.1% active chloride from NaOCl). After a 50-minute incubation, absorbance was measured at 630 nm using a micro plate reader (Molecular Device, USA). All experiments were conducted in triplicate, resulting in a total volume of 200 µL per well. The change in absorbance over time was analyzed with SoftMax Pro software (Molecular Device, USA). The assays were performed at pH 8.2 using a buffer solution containing 0.01 M $K_2HPO_4 \cdot 3H_2O$, 1 mM EDTA and 0.01 M $LiCl_2$. Thiourea served as the standard inhibitor for urease in this study

Urease Percentage inhibitions formula:

$$\% \text{ inbibition} = 100 - \left(\frac{\text{mean OD of Test well}}{\text{Mean O D of standard inhibitor}}\right) \times 100$$

Method of Urease inhibition of PDPC-stabilized AgNPs-doped TiO_2NPs

The reaction mixtures were created by mixing 25µL of Jack bean urease solution with 55µL of buffer and 100 mM urea. These mixtures were then incubated with 5µL of 1 mM PDPC-stabilized AgNPs-doped TiO_2NPs test compounds at 30°C for 15 minutes in 96-well plates. Urease activity was evaluated by measuring ammonia production using the indophenol method outlined by Weatherburn. Each well received 45 µL of phenol reagent (consisting of 1% w/v phenol and 0.005% w/v sodium nitroprusside) and 70µL of alkali reagent (made of 0.5% w/v NaOH and 0.1% active chloride from NaOCl). After a 50-minute incubation, absorbance was measured at 630 nm using a micro plate reader (Molecular Device, USA). All experiments were conducted in triplicate, resulting in a total volume of 200 µL per well. The change in absorbance over time was analyzed with SoftMax Pro software (Molecular Device, USA). The assays were performed at pH 8.2 using a buffer solution containing 0.01 M $K_2HPO_4 \cdot 3H_2O$, 1 mM EDTA and 0.01 M $LiCl_2$. Thiourea served as the standard inhibitor for urease in this study

Urease Percentage inhibitions formula

$$\% \text{ inbibition} = 100 - \left(\frac{\text{mean OD of Test well}}{\text{Mean O D of control}}\right) \times 100$$

Method of DPPH radical scavenging activity of PDPC-stabilized AgNPs-doped TiO_2NPs

The assessment of free radical scavenging activity was carried out using the 1,1-diphenyl-2-picryl-hydrazyl (DPPH) assay following the method outlined by Gulcin *et al*.,[26]. A 0.3 mM PDPC solution was prepared in EtOH. Various concentrations (62.5 to 500 mg) of PDPC-stabilized AgNPs-doped TiO_2NPs**.** samples were mixed with 95 µL of DPPH solution in ethanol. This mixture was then placed in a 96-well plate and incubated at 37°C for 30 minutes. The absorbance at 515 nm was measured using a microtiter plate reader (Spectramax Plus 384 from Molecular Devices, USA). The percentage of radical scavenging activity was determined by comparing the results to a methanol-treated control, with BHA serving as the standard reference.

PDPC -stabilized AgNPs-doped TiO_2NPs scavenging effect.
(%) = Ac – As/Ac × 100
Where
Ac = Absorbance of Control (DMSO treated)
As = Absorbance of Sample

Method of para-nitrophenol (PNP) reduction by PDPC-stabilized AgNPs-doped TiO_2NPs

In an aqueous solution, catalytic reduction of para-nitrophenol (PNP) was conducted in a quartz cuvette with a path length of 1 cm. In this cuvette, while stirring vigorously, 2.0 mL of a 0.125 mM PNP solution was combined with 4 mL of freshly prepared 5 M $NaBH_4$ solution. Subsequently, 400 µL of a 12.5 mM PDPC-stabilized AgNPs-doped TiO_2NPs catalyst was swiftly added. Within just one second, the solution changed color from dark yellow to colorless. The evolution of the reaction was monitored by recording UV-visible absorption spectra at one-second intervals across a 200 to 1000 nm wavelength range at ambient temperature.

Method of methylene-blue (MB) reduction by PDPC-stabilized AgNPs-doped TiO_2NPs

The reduction of methylene blue through catalysis was achieved using a system of PDPC-stabilized silver nanoparticles doped into titanium dioxide nanoparticles. In a Quartz Cell, freshly prepared solution of Methylene-blue dye (0.1mM; 2ml) was added under vigorous stirring. To this solution freshly prepared sodium borohydride solution ($NaBH_4$) (1M, 1ml) was added and then PDPC-stabilized AgNPs-doped TiO_2NPs system (50µL) was added immediately. The sample transitioned from dark blue to colorless within one second. The UV-visible absorption spectra were recorded to monitor the reaction progress at one-second intervals, covering a 200 to 1000 nm at room temperature.

STATISTICAL ANALYSIS

A statistical evaluation was performed on all values shown in the tables, with results reported as the standard error of the mean (± SEM) from three repeated tests. The change in absorbance over one minute was analyzed using SoftMax Pro software from Molecular Devices, USA.

RESULTS

Synthesis of 5-(-3-nitrophenyl)-3-(-pyridin-2-yl)-4,5-dihydro-1H-pyrazole-1-thioamide (PDPC)

Azachalcone was synthesized using a single step method outlined in Scheme 1. Initially, 3-nitrobenzaldehyde and 2-acetylpyridine were reacted in the presence of NaOH and methanol at 0 °C to synthesize (E)-3-(3-nitrophenyl)-1-(pyridin-2-yl)-prop-2-en-1-one which is known as Claisen-Schmidt condensation reaction. Subsequently, hetero-cyclization was performed on azachalcone to produce a pyrazole derivative known as 5-(-3-nitrophenyl)-3-(-pyridin - 2 - yl) - 4,5- dihydro - 1 H-pyrazole - 1 -thioamide (PDPC) via refluxing in absolute ethanol with potassium hydroxide and thiosemicarbazide.

The advancement of the reaction and the purity of the compounds were assessed using thin layer chromatography (TLC).

The pure product was isolated by washing the crude material with distilled water and then undergoing crystallization from ethanol. The structure of the synthesized compound was characterized using EI-MS and ^{1}H-NMR techniques.

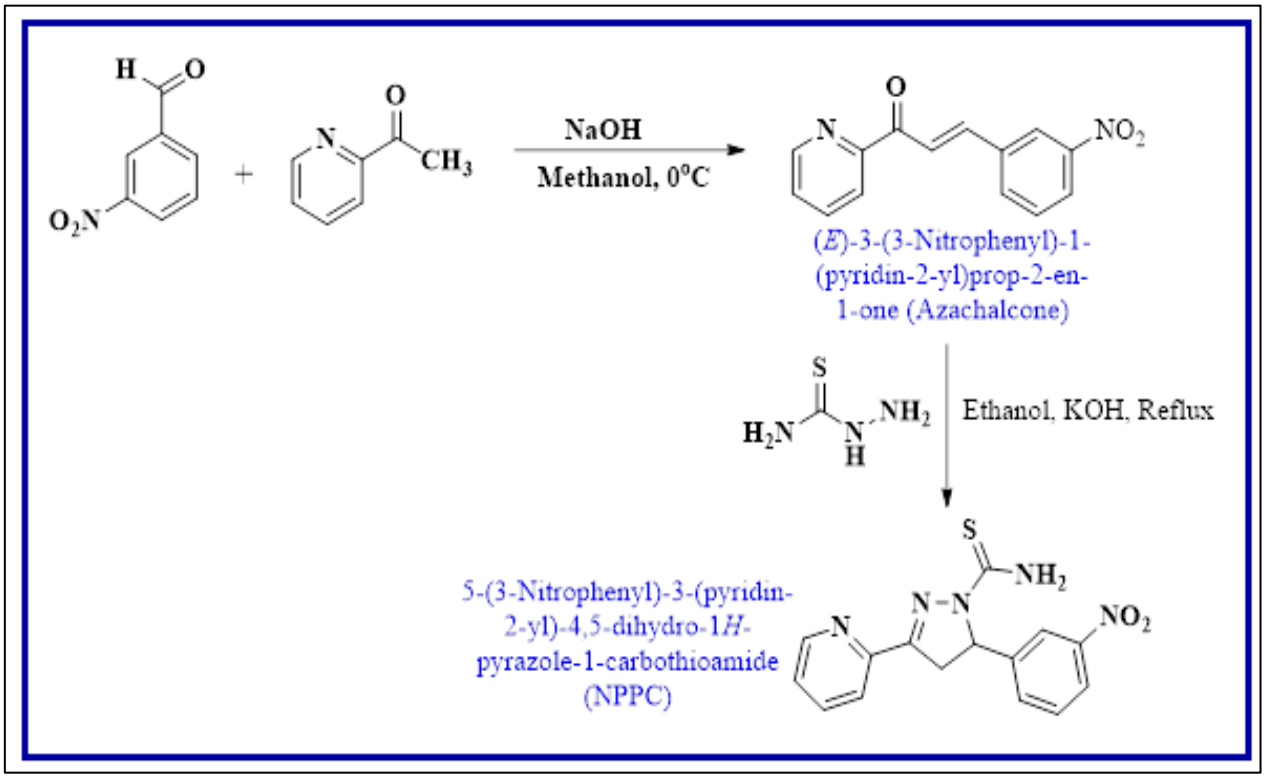

Scheme 1: Synthesis of 5-(-3-nitrophenyl)-3-(-pyridin-2-yl)-4,5-dihydro-1H-pyrazole-1-thioamide (PDPC)

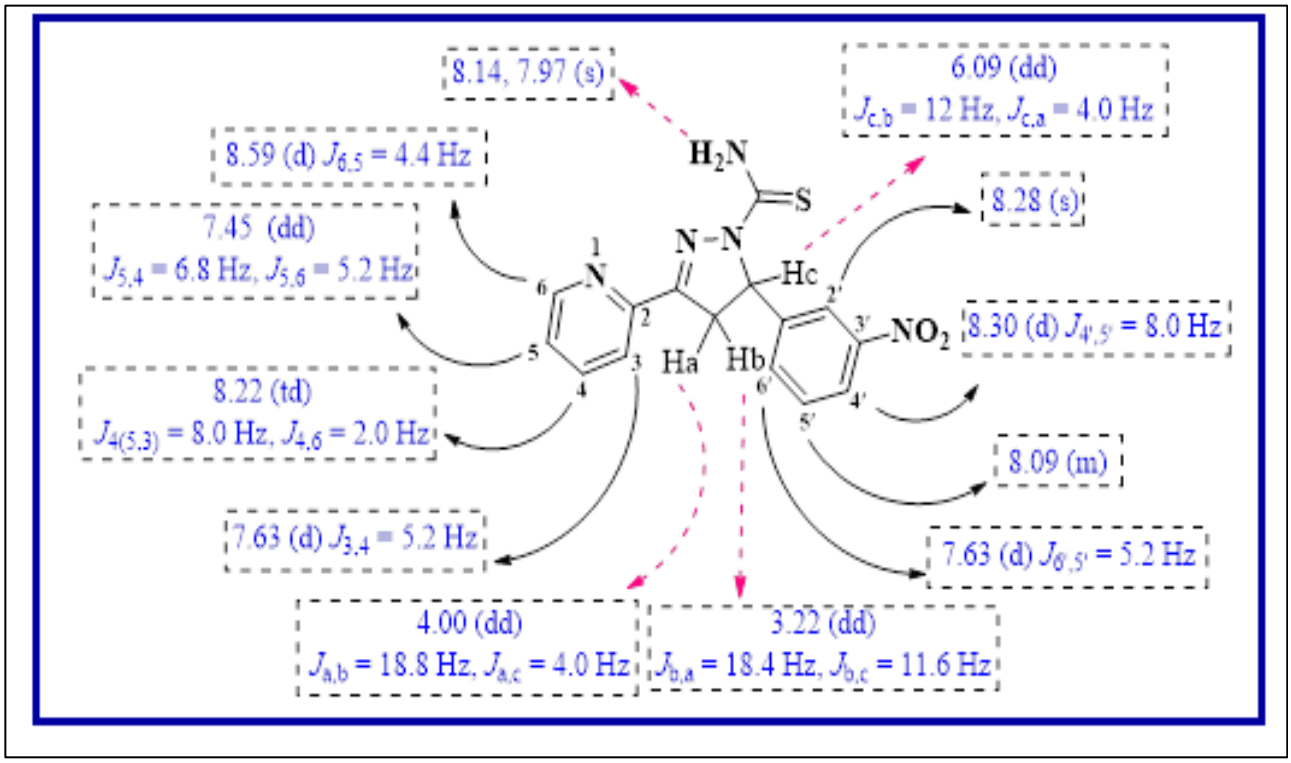

Fig. 1: 1H-NMR spectrum of PDPC

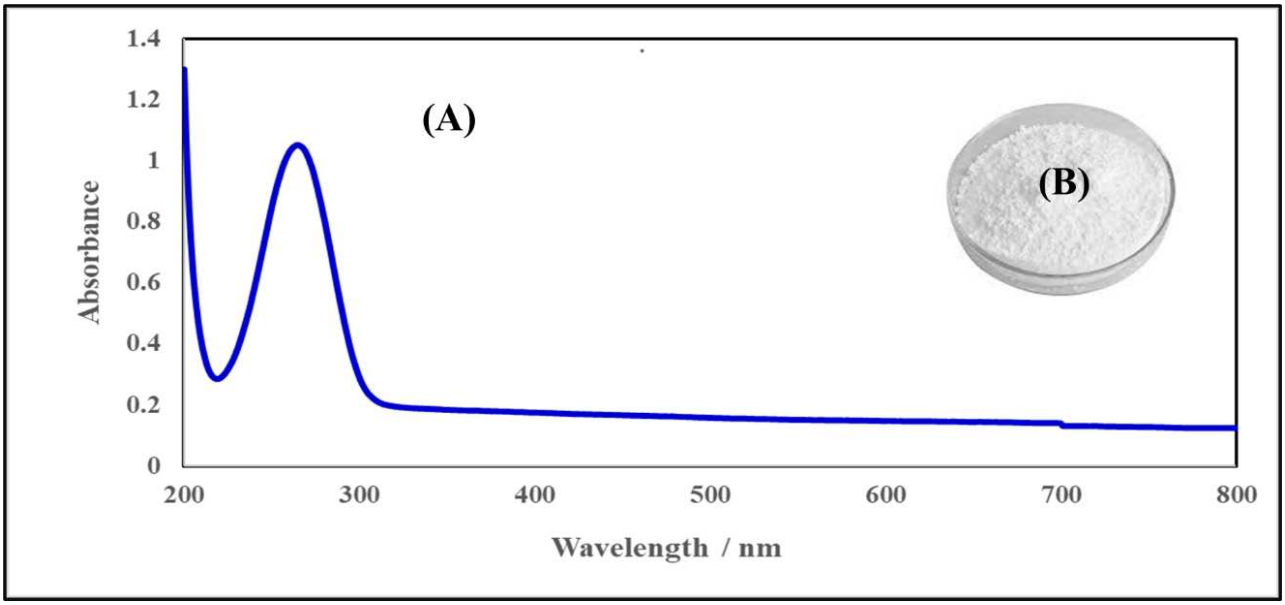

Fig. 2: (A) UV-visible absorption spectra of PDPC -TiO_2NPs system. λmax = 280 nm. (B) The white powder of PDPC-TiO_2NPs systems.

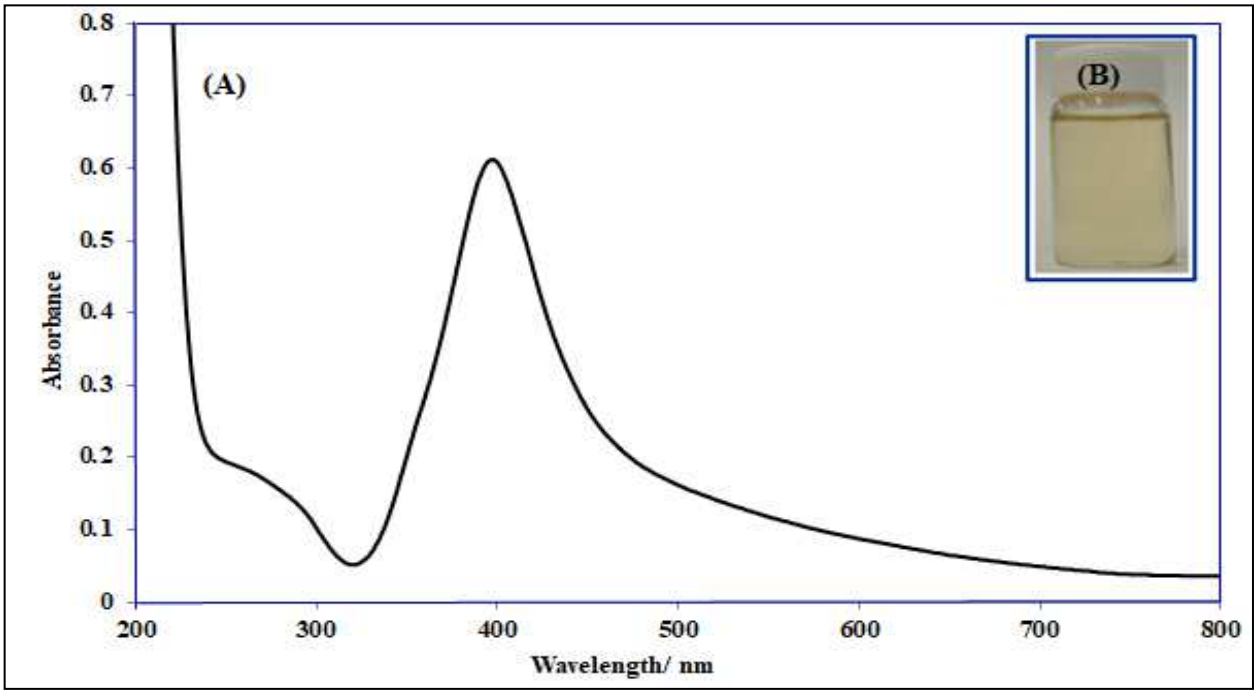

Fig. 3: **(A)** UV-Visible absorption spectra of PDPC-AgNps system, λmax = 405 nm (B) the yellow color of the PDPC-AgNps system.

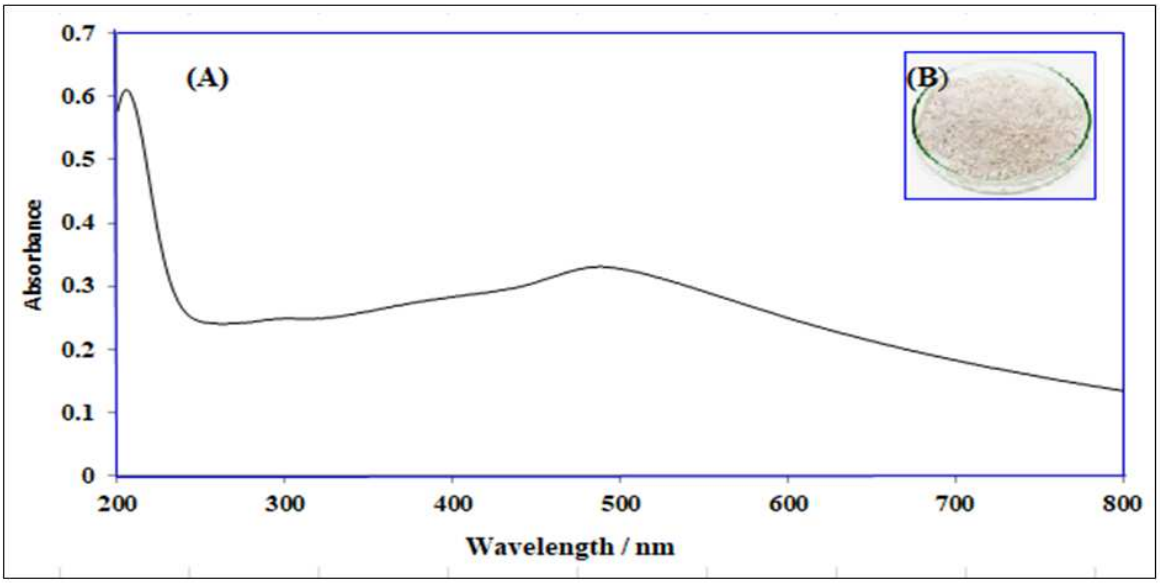

Fig. 4: (A) UV-Visible absorption spectra of AgNPs-doped TiO_2NPs-PDPC system. λmax = 490 nm. (B) The white powder of AgNPs-doped TiO_2NPs-PDPC system.

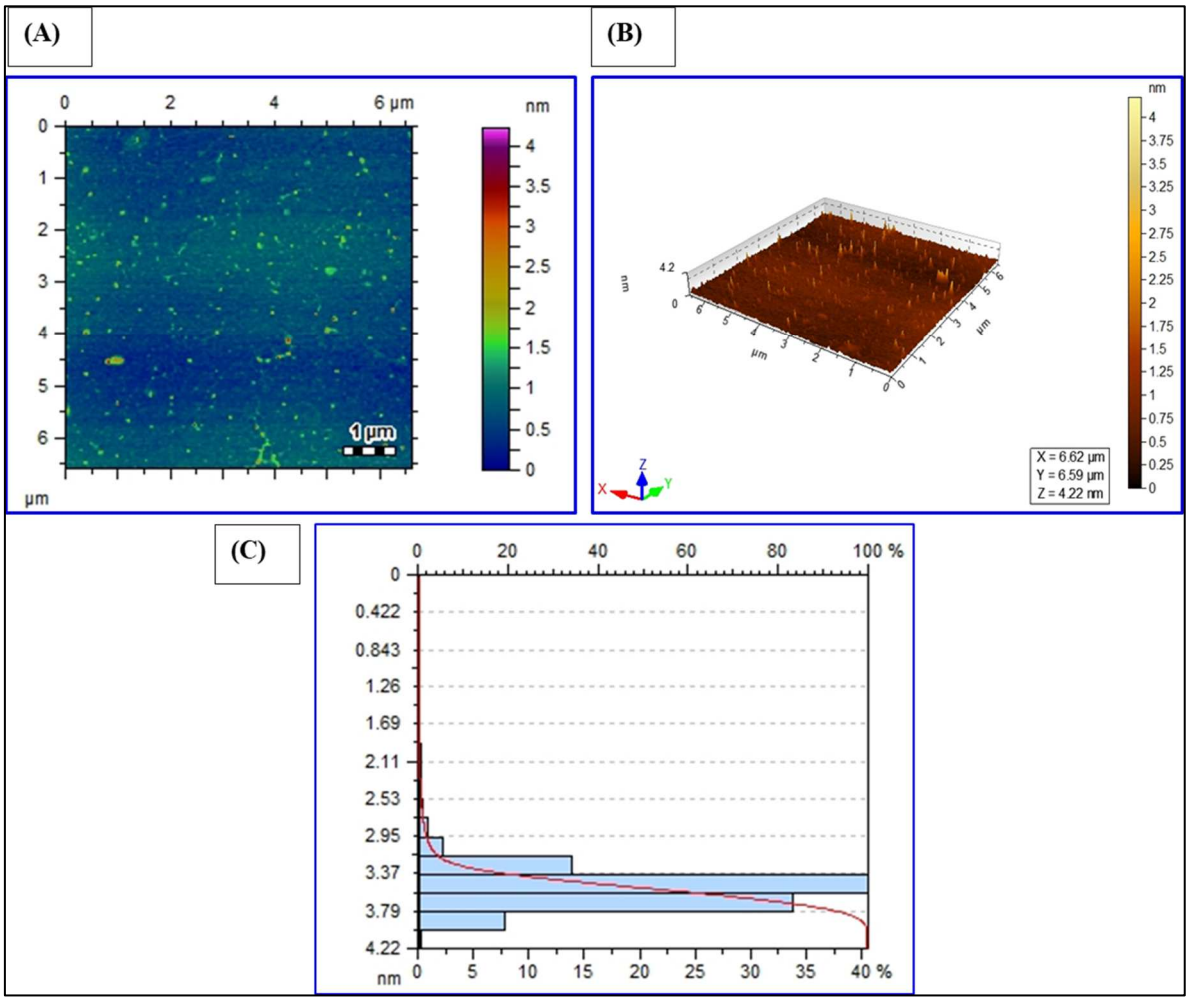

Fig. 5: (A, B) AFM images of PDPC-stabilized AgNPs-doped TiO_2NPs system. (C) Histogram of the corresponding size distribution of PDPC-stabilized AgNPs -doped TiO_2NPs system.

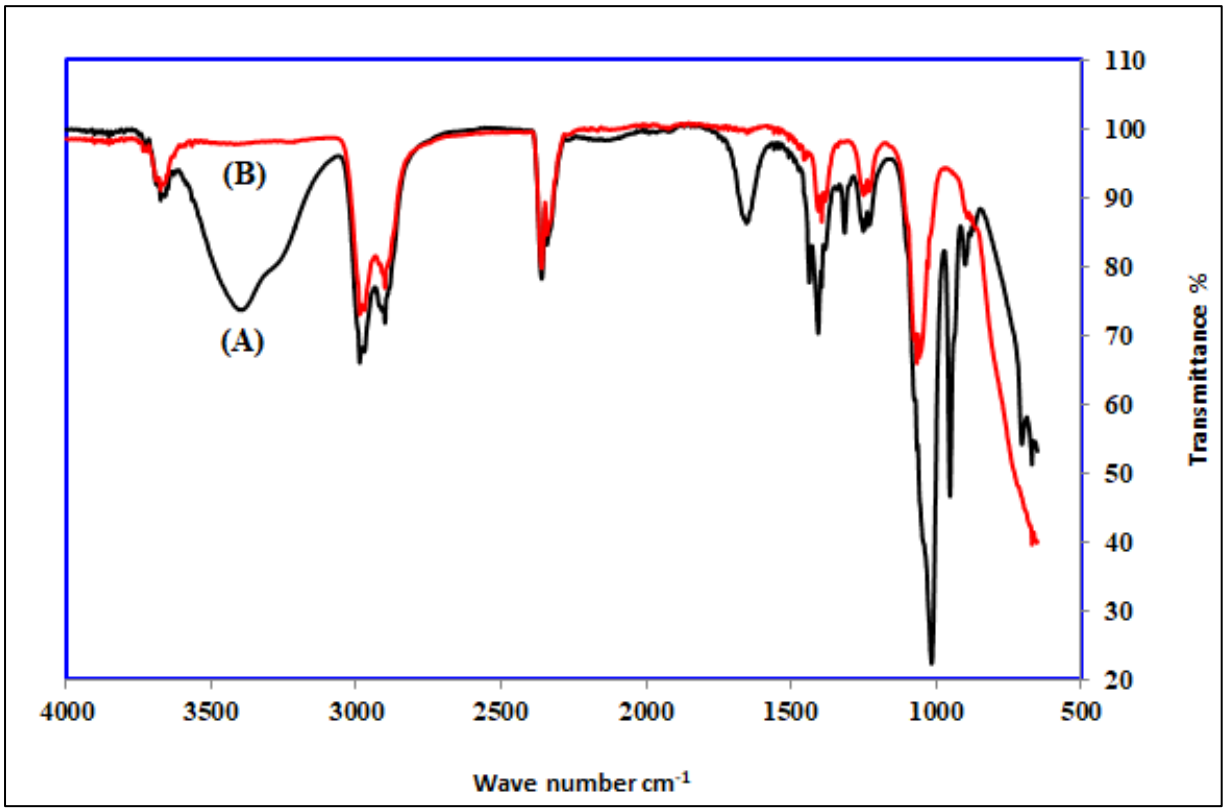

Fig. 6: (A) FTIR spectra of pure PDPC. (B) FTIR spectra of PDPC-stabilized AgNPs-doped TiO_2NPs systems.

Table 1: Urease inhibition activity of PDPC-stabilized AgNPs-doped TiO_2NPs system

S. No.	Compound	% Inhibition
1.	PDPC (control)	60 ± 0.92
2.	PDPC-AgNPs-doped TiO_2NPs	80 ± 0.53
3.	Standard = Thiourea	74 ± 0.82

Table 2: Antioxidant inhibition activity of PDPC-stabilized AgNPs-doped TiO_2NPs system

S. No.	Compound	% Inhibition
1.	PDPC (control)	35 ± 0.55
2.	PDPC-AgNPs-doped TiO_2NPs	82 ± 0.01
3.	Standard = Butylated Hydroxyanisole (BHA)	79 ± 0.90

Structural characterization of 5-(-3-nitrophenyl)-3-(-pyridin-2-yl)-4,5-dihydro-1H-pyrazole-1-thioamide (PDPC).

The Bruker Avance AM 400 MHz instrument was used to record the 1H-NMR spectrum of PDPC in deuterated DMSO-d6. The PDPC comprises a pyrazole ring, a 3-nitrophenyl ring and a 2-pyridyl ring. Among the 2-pyridyl ring, the H-6 proton being the most downfield at δ 8.59, split as a doublet due to o-coupling with H-5. H-4 appeared at δ 7.91 as a triplet of doublet because of o-coupling with H-3 and H-5 and m-coupling with H-6. H-3 resonated at δ 7.63 as a doublet; due to o-coupling with H-4, while H-5 appeared as a double doublet at δ 7.46 due to o-coupling with H-4 and H-6. The 3-nitrophenyl ring contains four protons with H-2′ and H-4′ appearing as singlet and doublet at δ 8.28 and 8.30, respectively. H-5′ appeared as a multiplet at δ 8.09, while H-6′ resonated as a doublet at δ 7.63. The pyrazole ring comprises three protons and the spectrum shows three signals. The characteristic peak of H-c appeared as double doublet due to 1,3-coupling with diastereotopic protons H-b and H-a at δ 6.09.

Furthermore, H-b and H-a resonated as double doublet due to 1,3 and 1,2-couplings at δ 4.00 and δ 3.22, respectively. Due to hydrogen bonding, the NH2 protons appeared as two broad singlets at δ 8.14 and δ 7.97. fig. 1: Provides a visual representation of these findings.

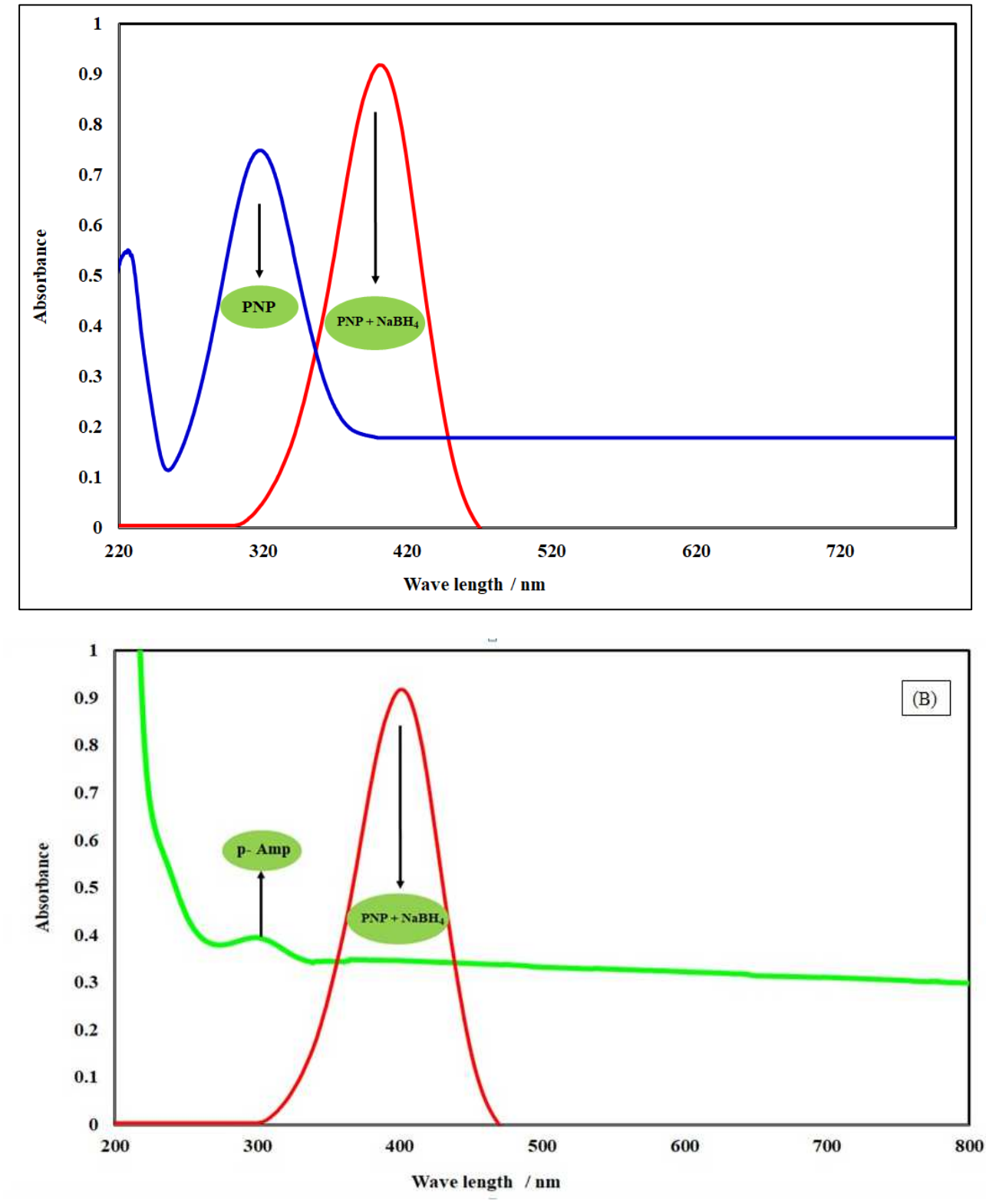

Fig. 7: (A) UV- visible absorption spectra of un-catalyzed reduction of para-nitrophenol (PNP) to para-nitrophenolate ion. (B) UV- Visible absorption spectra of reduction of para- nitrophenol (PNP) to para-aminophenol (p-Amp) in the presence of catalyst PDPC-stabilized AgNPs-doped TiO_2NPs system.

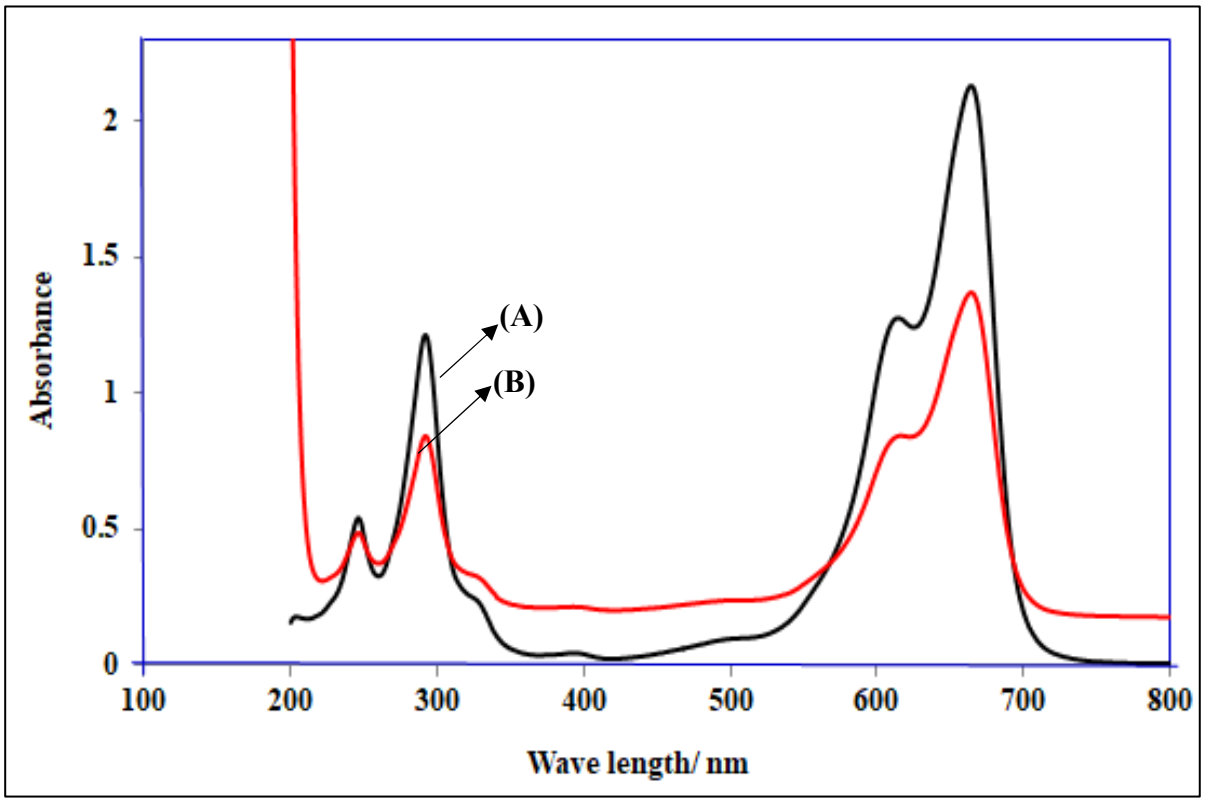

Fig. 8(A): UV-visible absorption spectra of un-catalyzed reduction of Methylene-blue (MB) **(B):** UV-visible absorption spectra of reduction of Methylene-blue (MB) after addition of $NaBH_4$.

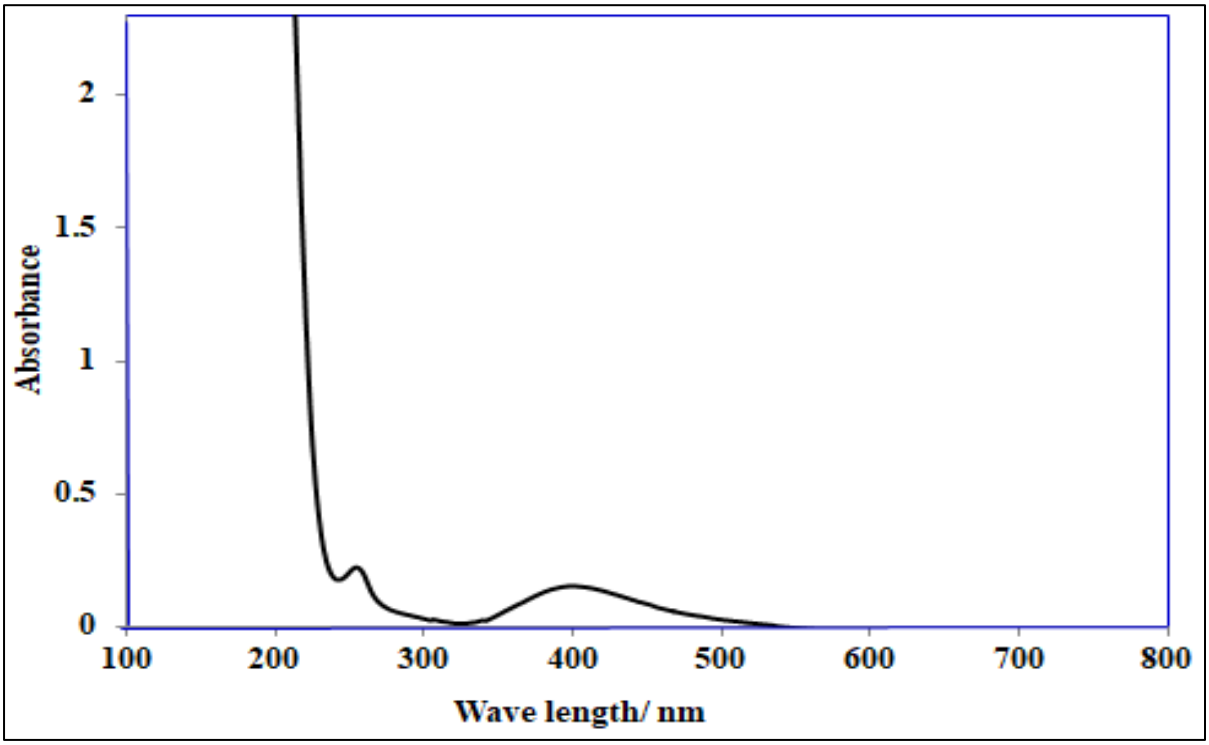

Fig. 8(C): UV-visible absorption spectra of reduction of Methylene-blue (MB) to leuco Methylene- blue (LMB) in the presence of catalyst PDPC-stabilized AgNPs-doped TiO_2NPs system.

Confirmation of PDPC-stabilized TiO_2NPs SPR by ultraviolet -visible spectroscopy

The formation of PDPC-stabilized TiO_2NPs is evidenced by surface plasmon resonance (SPR), which is supported by the Ultra violet-visible absorption spectra. The absorption spectrum in the UV-visible range for TiO_2NPs stabilized with PDPC, revealed a distinctive and intense surface plasmon resonance (SPR) band located at approximately 280 nm, as illustrated in fig. 2: (A). The presence of the SPR band confirms the existence of PDPC-stabilized TiO_2NPs, which stimulates the SPR effect. fig. 2: (B) clearly illustrates the white powder form of PDPC-stabilized TiO_2NPs.

Confirmation of PDPC-stabilized AgNPs SPR by UV-visible spectroscopy

The transparent precursor $AgNO_3$ and stabilizer PDPC solution turned yellow after adding $NaBH_4$ under slow stirring. The UV- visible absorption maxima of surface plasmon resonance (SPR) of AgNPs at 405 nm is demonstrated in fig. 3: (A). The solution continues to exhibit a yellow color indicates the formation of PDPC-stabilized AgNPs fig.3: (B).

Confirmation of PDPC-stabilized AgNPs doped TiO_2NPs SPR by UV-visible spectroscopy

The yellowish solution of PDPC-AgNPs was added under fast stirring in to transparent PDPC-TiO_2NPs system to form the PDPC-stabilized AgNPs doped TiO_2NPs. The UV- visible absorption maxima of surface plasmon resonance (SPR) band fig. 4: (A) of PDPC-stabilized AgNPs doped TiO_2NPs at about λmax = 490 nm. fig. 4: (B) clearly illustrates the white powder form of PDPC-stabilized AgNPs doped TiO_2NPs.

Surface morphology PDPC-stabilized AgNPs-doped TiO_2NPs by AFM

Furthermore, the shape, size and growth of PDPC-stabilized AgNPs-doped TiO_2NPs were confirmed by AFM images fig. 5: (A, B). The AFM images correlated well with the time-dependent observations from UV-visible spectroscopy. These images of the PDPC-stabilized AgNPs-doped TiO_2NPs systems demonstrated a consistent spherical shape and homogenous dispersion throughout the samples. The average particle sizes of the PDPC-stabilized AgNPs-doped TiO_2NPs system were 3 + 1 nm fig.5: (C).

FTIR analysis of PDPC-stabilized AgNPs-doped TiO_2NPs system

FTIR spectroscopy was conducted to verify whether PDPC had undergone chemisorption or physisorption with PDPC stabilized AgNPs-doped TiO_2NPs. A comparison of the spectra of pure PDPC in fig.6: (A) and PDPC-stabilized AgNPs-doped TiO_2NPs in fig. 6: (B) highlighted the interactions between PDPC and AgNPs-doped TiO_2NPs.

In PDPC-stabilized AgNPs-doped TiO_2NPs systems fig.6:(B), the N-H at resonance at 3400 cm^{-1}, strong, sharp peak in the 1700-1600 cm^{-1} range and C-S vibration at 900 cm^{-1} are absent. It suggests the carbothioamide bond is broken upon binding to the AgNPs-doped TiO_2NPs surface.

Anti-Urease activity of PDPC-stabilized AgNPs-doped TiO2NPs system

Our prepared PDPC-stabilized AgNPs-doped TiO_2NPs demonstrated notable inhibitory activity against the urease enzyme, as indicated by the percentage inhibition observed (% of inhibition 80 ± 0.53%) as compared to control PDPC (% of inhibition 60 ± 0.92) and standard Thiourea providing (% of inhibition =74 ± 0.82)

Anti-oxidant activity of PDPC-stabilized AgNPs-doped TiO_2NPs system

Our prepared PDPC-stabilized AgNPs-doped TiO_2NPs systems showed remarkable inhibitory antioxidant activity (% of inhibition 82 ± 0.01%) as compared to the control PDPC (control) 35 ± 0.55 and standard butylated hydroxyanisole (BHA) (% of inhibition 79 ± 0.90 %)

Heterogenous catalytic activity of PDPC-stabilized AgNPs-doped TiO_2NPs system for Para-nitrophenol (PNP) reduction

To evaluate the catalytic activity of PDPC-stabilized (AgNPs) doped into TiO_2NP***s***, we chose the reduction of para-nitrophenol (PNP) to para-aminophenol (p-Amp) as a suitable model reaction. This reaction is especially beneficial as it can be easily monitored using UV-visible spectroscopy (Vladimir Lomonosov *et al.,* 2022).

The Ultraviolet-Visible (UV-Vis) absorption spectrum of para-nitrophenol (PNP) observed at 323 nm shifted to 404 nm following the introduction of sodium borohydride ($NaBH_4$), indicating the formation of the para-nitrophenolate ion (fig. 7: A). Notably, the optical absorption spectrum of the reaction mixture remained unchanged after 48 hours, suggesting the stability of the para-nitrophenolate ion. To facilitate the conversion of this ion into para-aminophenol (p-Amp), an effective catalytic system is required to overcome the significant energy barrier posed by the similarly charged borohydride and para-nitrophenolate ions. Upon the addition of our synthesized heterogeneous catalyst, a PDPC-stabilized system of (AgNPs) infused into TiO_2NPs, we achieved the complete reduction of the para-nitrophenolate ion in just one second, as monitored by UV-visible optical spectroscopy (fig. 7: B). This rapid reaction was confirmed by the complete disappearance of the absorption peak at 404 nm associated with the para-nitrophenolate ion, coupled with the emergence of a new peak at 303 nm corresponding to para-aminophenol (p-Amp).

Heterogenous Catalytic activity of PDPC-stabilized AgNPs-doped TiO_2NPs ***system for Methylene-blue (MB) reduction***

Methylene-blue (MB) is a well-known azo dye that can be reduced to its colorless form leuco Methylene-blue (LMB),

using a reducing agent and a catalyst. Due to its enhanced catalytic activity the PDPC-stabilized AgNPs-doped TiO_2NPs system reduced MB to LMB. The reduction of Methylene-blue (MB) to leuco Methylene-blue (LMB) by PDPC-stabilized AgNPs-doped TiO_2NPs can occur *via* a similar mechanism comparable to the transformation of p-Nip into p-Amp.

The reaction can be monitored using UV-visible spectroscopy (fig. 8(A) by measuring the reduction of MB at 669 nm and after addition of $NaBH_4$ at 664 nm (fig. 8(B) with time and the appearance of a new absorbance peak within one sec of leuco Methylene-blue (LMB) at 387 nm (fig. 8(C).

This enhancement is likely driven by the increased surface area of the AgNPs, which provides more active sites for the reaction to take place. In addition, the TiO_2NPs act as a support for the AgNPs and also provide additional catalytic activity due to their photocatalytic properties.

DISCUSSION

The surface plasmon resonance (SPR) in TiO_2NPs arises from the collective oscillation of electrons on the surface of the nanoparticles, which are excited by light. Specifically, when light is incident on the surface of the TiO_2NPs it creates an electromagnetic field that interacts with the electrons on the surface of the particles. This interaction causes the electrons to oscillate collectively, resulting in the surface plasmon resonance. Generally, the SPR of TiO_2NPs is observed in the range of 250-450 nm in the UVB and UVC regions of the electromagnetic spectrum. fig. 2: (A) exhibited the signature strong SPR band of TiO_2NPs at about 280 nm. fig. 2: (B) clearly illustrates the white powder form of PDPC-stabilized TiO_2NPs Moreover, in the synthesis of PDPC-stabilized AgNPs, sodium borohydride ($NaBH_4$) was employed to reduce silver ions (Ag^+) to elemental silver (Ag^0). Following the gradual addition of $NaBH_4$ to a transparent solution of $AgNO_3$ and PDPC stabilizer, the mixture turned into a lasting yellow color. This stable yellow coloration serves as an indication of the stabilization of the resulting AgNPs by PDPC. This stabilization was confirmed by observing the distinctive surface plasmon resonance (SPR) absorption peak observed at 405 nm, as illustrated in fig. 3: (A). As illustrated in fig. 3: (B). The stable yellow color of the solution confirms the successful synthesis of PDPC-stabilized AgNPs. Doping the as-prepared PDPC-stabilized AgNPs into PDPC-stabilized TiO_2NPs can be achieved by adding the yellowish PDPC-AgNPs solution to the transparent PDPC- TiO_2NPs system under vigorous stirring. This results in the formation of PDPC-stabilized AgNPs-doped TiO_2NPs. The UV-visible absorption maxima of surface plasmon resonance (SPR) band fig. 4: (A) of PDPC-stabilized AgNPs doped TiO_2NPs at about λmax = 490 nm. The redshift in the absorption peak can also be affected by various factors such as the size, shape and the concentration of the AgNPs dopant. fig. 4: (B) clearly illustrates the white powder form of PDPC-stabilized AgNPs doped TiO_2NPs (Sijia Lv *et al.,* 2022).

The characteristic sharp UV-visible fig. 4: (A,B) SPR band of PDPC-stabilized AgNPs-doped TiO_2NPs indicated the synthesis of stable, spherical and uniformly sized, small nanoparticles, also demonstrated in the AFM micrographs fig.5: (A, B). The mean size of the PDPC-stabilized AgNPs doped TiO_2NPs was determined to be 3 ± 1 nm in fig.5: (C).

FTIR spectroscopy was utilized to explore the interactions between stabilizers (PDPC) and the surface of AgNPs-doped TiO_2NPs, along with any potential conformational changes. The appearance of new bands and alterations in existing bands indicated that PDPC was binding to the AgNPs-doped TiO_2NPs. Furthermore, in pure PDPC, fig.6: (A) depicts a broad peak associated with N-H stretching vibrations at approximately 3400 cm^{-1}. C–H aromatic stretching and both in-plane and out-of-plane bending vibrations were observed in the frequency ranges of 3000-2900 cm^{-1} and 1400-1100 cm^{-1}respectively. A sharp strong peak corresponds to stretching vibrations of the aromatic ring (C=C) found in the range of 1600-1700 cm^{-1} Additionally, a moderate peak around 1000-1200 cm^{-1} corresponds to the vibrational stretching of the C-N bond, while a moderate peak for C-S stretching vibrations is found at approximately 900 cm^{-1}.

In the PDPC-stabilized AgNPs-doped TiO_2NPs systems demonstrated in fig. 6 (B) the NH resonance peak at 3400 cm^{-1}, the strong, sharp peak in the 1700-1600 cm^{-1} range and the C-S vibration at 900 cm^{-1} are absent.

This indicates that the carbothioamide bond is cleaved during its binding with the surface of PDPC-stabilized AgNPs-doped TiO_2NPs. Additionally, the observed shifts of the other frequencies to lower values suggest a compact, rigid packing of PDPC around the AgNPs-doped TiO_2NPs (Pasieczna-Patkowska, S *et al.,* 2025)

The urease inhibitory activity of PDPC-stabilized AgNPs-doped TiO_2NPs refers that these nanoparticles inhibit the activity of the urease enzyme. Urease enzyme is found in bacteria and contributes to the process of urea hydrolysis, which can lead to the production of ammonia and other harmful substances. Therefore, to assess the potential biological uses of PDPC-stabilized AgNPs-doped TiO_2NPs, a urease inhibition was conducted using the urease enzyme extracted from jack beans. The results indicated that our PDPC-stabilized AgNPs-doped TiO_2NPs systems demonstrated meaningful inhibitory activity against the urease enzyme, with a % inhibition of 80 ± 0.53%. It contrasts the control thiourea, (Asadi, S *et al.,* 2025) which provided a % inhibition of 74 ± 0.82% (table 1).

The antioxidant activity of PDPC-stabilized AgNPs-doped TiO_2NPs is another active research area. Antioxidants play a role in shielding cells from damage inflicted by reactive oxygen species produced due to normal cellular metabolism or exposure to environmental stressors. Recent research has indicated that PDPC-stabilized AgNPs doped into TiO_2NPs possess antioxidant properties and may find potential uses in diverse areas such as healthcare, personal care products and food safety. The mechanism of their antioxidant activity is believed to be due to the capability of the nanoparticles to capture free radicals or function as electron donors, thereby reducing oxidative stress and preventing cellular damage. Our synthesized PDPC-stabilized AgNPs-doped TiO_2NPs systems demonstrated significant antioxidant activity, with an inhibition rate of 82 ±0.01%. In contrast, the standard butylated hydroxyanisole (BHA) exhibited (Balkrishna, A *et al.,* 2021) an inhibition rate of 79 ± 0.90% (table 2).

To showcase our systems PDPC-stabilized AgNPs-doped TiO_2NPs, we focused on the transformation of intense yellowish solution of para-nitrophenol (PNP) into colorless, para-aminophenol (p-Amp). Initially, the concentration of $NaBH_4$ was set at 0.5 M and remained unchanged throughout the course of the reaction, while the p-nitrophenol concentration was set at 0.125 mM. As exhibited in fig. 7 (A), the UV-visible spectra illustrate this reduction process. With the aid of our synthesized heterogeneous catalyst, which consists of PDPC-stabilized AgNPs doped into TiO_2NPs, along with sodium borohydride ($NaBH_4$), the reduction of para-nitrophenol occurred. In fig. 7 (B), the absorption maximum at 404 nm quickly diminished within one second and simultaneously, a new peak at 303 nm appeared, indicating the formation of para-aminophenol (p-Amp).

To further assess an application of PDPC-stabilized AgNPs doped TiO_2NPs as heterogeneous catalyst, we employed pseudo-Ist-order rate kinetics concerning p-nitrophenol, given the significantly higher concentration of $NaBH_4$ in comparison to that of p-nitrophenol.

The reduction of Methylene-blue (MB) to form leuco Methylene-blue (LMB) by PDPC-stabilized AgNPs-doped TiO_2NPs can also occur via a similar reduction mechanism as of para-nitro phenol (PNP) to para-aminophenol (p-amp). Methylene-blue (MB) is a well-known toxic azo dye capable of being reduced to its colorless form, leuco Methylene-blue (LMB), using a reducing agent and a catalyst. In this case, the catalyst being studied is the PDPC-stabilized AgNPs-doped TiO_2NPs system. The reaction can be monitored through UV-visible spectroscopy fig. 8: (A) by tracking the reduction in the absorbance of methylene blue (MB) at 669 nm as time progresses (Adeleye, A.T *et al.,* 2022).

After addition of reducing agent ($NaBH_4$) in aqueous MB solution, the UV-visible absorption peak reduced to 664 nm fig. 8: (B) after addition of PDPC-stabilized AgNPs-doped TiO_2NPs the peak at 664 nm will disapperared with in one second and new absorbance peak of leuco Methylene-blue (LMB) at 387 nm (fig. 8 (C) appeared. The PDPC-stabilized AgNPs-doped TiO_2NPs system is expected to enhance the catalytic reduction reaction rate compared to TiO_2NPs - alone due to the doping effects of AgNPs. The mechanism behind this enhancement is likely due to the increased S/A ratio of the AgNPs, which confirms the availability of more active sites for the reaction to occur. In addition, the TiO_2NPs act as a support for the AgNPs and also provide additional catalytic activity due to their photocatalytic properties.

CONCLUSION

This study presents a detailed methodology for synthesizing stable AgNPs doped TiO_2NPs using a novel short-chain stabilizer, 5-(3-Nitrophenyl) Hydrazono-2-Pyridine-4,5-Dihydro-1H-Pyrazole-1-Thioamide (PDPC). All experiments conducted under ambient temperature and pressure, the resulting PDPC-stabilized AgNPs-doped TiO_2NPs were characterized by their spherical shape and mean diameter of 3 ± 1 nm, as confirmed by atomic force microscopy (AFM). The synthesized PDPC-stabilized AgNPs-doped TiO_2NPs demonstrated exceptional heterogeneous catalytic activity. They effectively facilitated the conversion through reduction of 4-nitrophenol (PNP) to 4-aminopheno (p-Amp) and Methylene-Blue (MB) to lecuo Methylene-Blue (LMB) in a second. Moreover, this system exhibited significant urease inhibitory and antioxidant properties, highlighting its versatility. The method used for synthesis is not only straightforward and cost-effective but also results in biocompatible and reproducible materials. These qualities position the PDPC-stabilized AgNPs-doped TiO_2NPs as promising candidates for various commercial and environmental applications, including wastewater treatment, biomedical uses and environmental remediation strategies. Their potential to enhance catalytic efficiency and support sustainability makes them a valuable addition to the field of nano materials.

ACKNOWLEDGMENT

The authors acknowledge the financial support of the Sindh Higher Education Commission (SHEC), Pakistan, *vide* letter No. NO.DD/SHEC/1-14/2014, Project code SHEC/SRSP/Med-3/15/2021-2.

Conflict of interest

The authors declare that there is no conflict of interest regarding the publication of this document.

REFERENCS

Caglar A, Kivrak H and Aktas N (2022). The effect of titanium dioxide-supported CdSe photocatalysts

Enhanced for photocatalytic glucose electrooxidation under UV illumination. *Int. J. Hydrogen Energy,* **47**(49): 21130-21145.

George J, Nath GR and Rajesh K (2022). Bis (2-Cyclooctylidenehydrazene-1-carbothioamide) Zinc (II), a good single source precursor for ZnS nanoparticles-Synthesis and crystal structure. *Results Chem*., **4**: 100601.

Giuseppe G, Graziantorio L, Alessia C, Alessia C, Maria SS and Neuroprotective. (2024) Effects of curcumin in neurodegenerative disease. *Food.,* **13**(11): 1774.

Grala M, Kołodziejczyk AM, Białkowska K, Walkowiak B and Komorowski P (2023). Assessment of the influence of gold nanoparticles stabilized with PAMAM dendrimers on HUVEC barrier cells. *Micron,* **168**: 103430.

Kianfar AH and Arayesh MA (2020). Synthesis, characterization and investigation of photocatalytic and catalytic applications of Fe_3O_4/TiO_2/CuO nanoparticles for degradation of MB and reduction of nitrophenols. *J. Environ. Chem. Eng*., **8**(1): 103640.

Kocić A, Bizjak M, Popović D, Poparić GB and Stanković SB (2019). UV protection is afforded by textile fabrics made of natural and regenerated cellulose fibres. *J. Clean. Prod.,* **228**: 1229-1237.

Liu JD, Feng Y, Zhao YY, Hu XM, Wu MY, Yu XX, Song CY, Zhu SC, FanYJ and Li WQ (2022). Effect of TiO_2-NPs on microbial-induced calcite carbonate precipitation. *J. Environ. Chem. Eng.,* **10**(1): 107041.

Luzia V Modolo, Cristiane J da-Silva, Débora S Brandão and Izabel S Chaves (2018). A minireview on what we have learned about urease inhibitors of agricultural interest since mid-2000s. *J. Adv. Res*., **17**(13): 29-37.

Madkour M, Bumajdad A and Al-Sagheer F (2019). To what extent do polymeric stabilizers affect Nanoparticle characteristics? *Adv. Colloid Interface Sci.*, **270**: 38-53.

Monti E, Ventimiglia A, Soto CAG, Martelli F, Rodríguez-Aguado E, Cecilia JA, Maireles-Torres P, Ospitali F, Tabanelli T, Albonetti S and Cavani F (2022). Oxidative condensation/esterification of furfural with ethanol using preformed Au colloidal nanoparticles. Impact of stabilizer and heat treatment protocols on catalytic activity and stability. *Mol. Catal.*, ***528***: 112438.

Muthukrishnan S, Vidya R and Sjåstad A (2023). Band gap engineering of anatase TiO2 by ambipolar doping: A first-principles study. *Mater. Chem. Phy.,* **299**(1): 127467.

Nagar A and Pradeep T (2020). Clean water through nanotechnology: Needs, gaps and fulfillment. *ACS Nano.*, **14**(6): 6420-6435.

Naidoo L, Kanchi S, Drexel R, Meier F and Bisetty K (2021). Measurement of TiO2 nanoscale Ingredients in sunscreens by multidetector AF4, TEM and spICP-MS supported by computational modeling. *ACS Appl. Nano Mater.*, **4**(5): 4665-4675.

Nilavukkarasi M, Vijayakumar S, Kalaskar M, Gurav N, Gurav S and Praseetha PK (2022). *Capparis zeylanica L*. conjugated TiO_2 nanoparticles as bio-enhancers for antimicrobial and chronic wound repair. *BBRC.*, **623**(1): 127-132.

Talebian S, Rodrigues T, Das Neves J, Sarmento B, Langer R and Conde J (2021). Facts and fig. on materials science and nanotechnology progress and investment. *ACS Nano.,* **15**(10): 15940-15952.

Thukkaram M, Cools P, Nikiforov A, Rigole P, Coenye T, Van Der Voort P, Du Laing G, Vercruysse C, Declercq H, Morent R and De Wilde L (2020). Antibacterial activity of a porous silver doped TiO_2 coating on titanium substrates synthesized by plasma electrolytic oxidation. *Appl. Surf. Sci.*, **500** (10): 144235.

Trinh TTPNX, Trinh DN, Cuong DC, Hai ND, Thinh DB, Hoa HN, Cong CQ, Nam NTH, An H, Khoa TD and Dai Viet VN (2023). Optimization of crystal violet photodegradation and investigation of the antibacterial performance by silver-doped titanium dioxide/graphene aerogel nanocomposite. *Ceram. Int.,* **49** (12): 20234-20250.

Waghmode MS, Gunjal AB, Mulla JA, Patil NN and Nawani NN (2019). Studies on the titanium dioxide nanoparticles: Biosynthesis, applications and remediation. *SN Appl. Sci.*, **1**(4): 310.

Yerli-Soylu N, Akturk A, Kabak O, Erol-Taygun M, Karbancioglu-Guler F and Küçükbayrak S (2022). TiO_2 nanocomposite ceramics doped with silver nanoparticles for the photocatalytic degradation of methylene blue and antibacterial activity against Escherichia coli. *Eng. Sci. Technol. Int. J.,* **35**(3):101175.

Zhu Y and Egap E (2021). Light-mediated polymerization induced by semiconducting nanomaterials: State-of-the-art and future perspectives. *ACS Polymers Au.*, **1**(2): 76-99.